Available online at www.sciencedirect.com
ScienceDirect
Journal of Power Sources 166 (2007) 590–594
JOURNAL OF POWER SOURCES
www.elsevier.com/locate/jpowsour

Short communication

In situ Mn K-edge X-ray absorption spectroscopic studies of anodically deposited manganese oxide with relevance to supercapacitor applications

Jeng-Kuei Chang *, Ming-Tsung Lee, Wen-Ta Tsai

Department of Materials Science and Engineering, National Cheng Kung University, 1 Ta-Hsueh Road, Tainan 701, Taiwan

Received 29 September 2006; accepted 12 January 2007
Available online 26 January 2007

Abstract

Fibrous morphology and nano-crystalline nature of the anodically deposited manganese oxide were confirmed by a transmission electron microscope (TEM). The oxide electrode exhibited an ideal capacitive behavior as indicated by cyclic voltammetry (CV). In order to explore the energy storage mechanism, variation of electronic and structural aspects of the manganese oxide induced by changing the applied potential was studied in situ in aqueous 2 M KCl by Mn K-edge X-ray absorption spectroscopy (XAS). Position shift of the adsorption edge, toward higher energy during oxidation and backward lower energy during reduction, was clearly recognized. The experimental results directly proved for the first time that the pseudo-capacitance of the manganese oxide was attributed to its continuous and reversible faradic redox reaction during the charge–discharge process.

Keywords: Manganese oxide; Pseudo-capacitance; Supercapacitor; X-ray absorption; In situ spectroscopy

1. Introduction

Electrochemical supercapacitors are charge-storage devices that have greater power density and longer cycle life than batteries, and possess higher energy density compared with conventional capacitors [1]. They have recently considered to be a favorable device in many fields, e.g. hybrid power sources, peak-power sources, backup-power storage, lightweight electronic fuses, starting power of fuel cells, etc. [2–4]. According to the operative manners, the supercapacitors can be classified into two different types: (1) double-layer capacitors, which are based on the non-faradic charge separation at an electrode/electrolyte interface, and (2) pseudo-capacitors, which are based on the faradic redox reaction of electro-active materials. Manganese oxide, owing to the satisfactory capacitance and its natural abundance and environmental compatibility, has been considered as one of the most promising electrodes for supercapacitor applications. However, the charge-storage mechanism of manganese oxide was not investigated in detail. A suggested mechanism has been proposed as follow [5–7]:

$$\mathrm{MnO}_a(\mathrm{OH})_b + n\,\mathrm{C}^+ + n\,\mathrm{e}^- \leftrightarrow \mathrm{MnO}_{a-n}(\mathrm{OH})_{b+n} \quad (1)$$

where C^+ denotes the alkali metal cation or proton in the electrolyte. Some researchers [6–8] believed that the C^+ can intercalate into the bulk oxide upon reduction followed by its deintercalation during oxidation. Nevertheless, others considered that only the chemisorption and desorption reactions occurred on the oxide surface [5,9,10]. In addition, how does the Mn valence state adjust during the electrochemical redox process has not yet been clearly certified. Undoubtedly, the understanding of the electrochemical mechanism associated with the pseudo-capacitive characteristics is a key factor to develop the supercapacitor electrodes displaying optimized performance, ex. high specific capacitance, high power capability, long cycle life, etc.

To explore the Mn oxidation state change during the electrochemical process became a crucial topic; however, few studies were reported due to the difficulty of monitoring. An ex situ X-ray photoelectron spectroscopy (XPS) study was performed by Toupin et al. [11] to examine the reduced and oxidized manganese oxide thin films (only two conditions), revealing the Mn oxidation states of +3 and +4, respectively. However,

* Corresponding author. Tel.: +886 6 2757575x62942; fax: +886 6 2754395.
E-mail address: catalyst@mail.mse.ncku.edu.tw (J.-K. Chang).

0378-7753/$ – see front matter © 2007 Elsevier B.V. All rights reserved.
doi:10.1016/j.jpowsour.2007.01.036

they also found that the oxidation state could change during drying and exposure to air. Especially for the thick oxide sample (dozens of micro-meters), the measured Mn oxidation state would most likely be averaged due to the chemical potential difference between the surface and the bulk material. On the other hand, Nakayama et al. [12] have also inspected the Mn oxidation state of the reduced and oxidized Mn/Mo mixed oxide in the same manner. Respective Mn valences of +3.6 and +4 for the two conditions were detected, which showed the much smaller difference of the oxidation state than that reported by Toupin et al. [11]. It should be noticed that the ex situ XPS experiment must be carried out in an ultra high vacuum chamber, and the analytic data can only provide the material's information from a very surface region (typically a few nanometers). Therefore, it might not be the most suitable tool to investigate the realistic valence variation. This study first demonstrated an in situ monitor in electronic and structural properties of the manganese oxide in aqueous KCl electrolyte as a function of the applied potential using X-ray absorption spectroscopy (XAS). Accordingly, the energy storage mechanism with relevance its pseudo-capacitance was also discussed herein.

2. Experimental

Manganese oxide was electroplated onto 1 cm × 1 cm graphite substrates by anodic deposition in a neutral 0.5 M $Mn(CH_3COO)_2$ plating solution at 25 °C. The substrates were first polished with grit 800 SiC paper, degreased with acetone and water, then etched in a 25 °C 0.2 M H_2SO_4 solution, and finally washed with pure water in an ultrasonic bath. During the deposition, a three-electrode electrochemical system was employed, and the graphite-working electrode was maintained as the anode. A platinum sheet and a saturated calomel electrode (SCE) were used as the counter electrode and the reference electrode, respectively. The deposition condition was controlled by an EG&G Princeton Applied Research model 263 potentiostat. The applied potential was constant at 0.5 V (versus SCE) to give a total passed charge of 1.5 C.

An ultra-thin sectioning technique was employed to prepare the TEM specimen of the manganese oxide. The detached manganese oxide was placed in a gelatin capsule containing Spurr's epoxy resin mix. The sample was then kept at 60 °C over 24 h for complete polymerization. Initially, the block of resin was trimmed with a steel knife, and then it was sectioned with a diamond cutter of an ultra-microtome. The section thickness was generally 40–60 nm. After cutting, the sections were mounted on copper grids and examined via TEM (Hitachi HF-2000) at 200 kV. A camera length of 100 cm was adopted as the electron diffraction was performed.

The electrochemical characteristics of the deposited manganese oxide were evaluated by cyclic voltammetry (CV) in 2 M KCl solution at 25 °C. Configuration of the electrochemical cell and the testing instrument were the same as those used for the anodic deposition. The potential was scanned at a rate of 20 mV s^{-1} within a range of 0–1 V (versus SCE). In situ X-ray absorption spectroscopic (XAS) studies under various applied potentials were carried out in the fluorescence mode. Fig. 1 shows the configuration of the spectro-electrochemical cell with a window sealed by the Kapton tape, which was fluorescence transparent. Twenty-one sequent XAS scans were acquired at different potentials with an interval of 0.1 V, starting from 0 to 1 V_{SCE} and then back to 0 V_{SCE}. The applied potentials were held constantly for 15 min before XAS analyses and during the whole acquisition (about 40 min) as well. The XAS experiment was performed at beam line 17C of the Synchrotron Radiation Research Center (SRRC) in Hsinchu, Taiwan. The storage ring was operated with an electron energy of 1.5 GeV and a current between 100 and 200 mA. A Si (1 1 1) double crystal monochromator was employed for energy selection. The XAS energy was calibrated using the first inflection point of the Mn K-edge region of a metallic Mn foil (6539 eV), which was measured simultaneously in each scan. Moreover, in order to identify the oxidation state of the deposited manganese oxide under various electrochemical conditions, MnO, Mn_2O_3 and MnO_2 compounds were used as the references in XAS analyses.

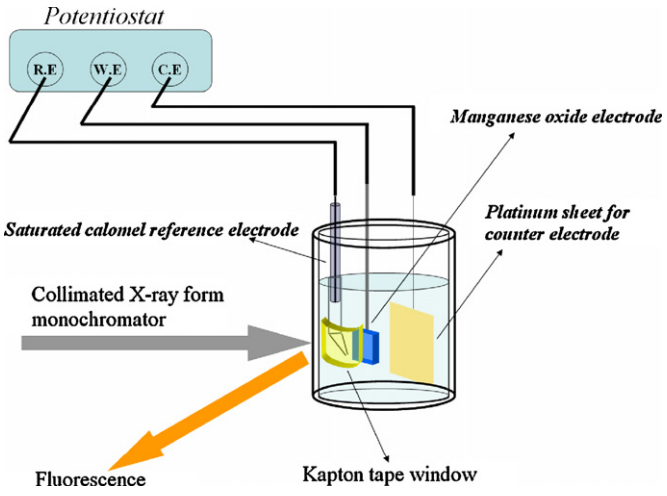

Fig. 1. Schematic diagram of the spectro-electrochemical cell for in situ XAS study in the fluorescence mode.

3. Results and discussion

Fig. 2(a) shows the TEM bright-field image of the manganese oxide prepared by anodic deposition, depicting that the deposit consisted of oxide fibers. The size of the fibers was generally several nanometers in diameter and tens nanometers in length. An electron diffraction pattern of the manganese oxide was taken and is shown in Fig. 2(b). Dim rings in the pattern revealed the nano-crystalline nature of the oxide. The deposited oxide was also found to be hydrous and non-stoichiometric in our previous reports [13,14]. Owing to the unique material characteristics, the manganese oxide can demonstrate an electrochemical property as shown in Fig. 3. This figure presents the cyclic voltammogram of the oxide electrode, measured in 2 M KCl aqueous electrolyte at 25 °C, at a potential scan rate of 20 mV s^{-1}. The CV curve was close to a rectangular shape and exhibited mirror-image characteristics, elucidating the ideal pseudo-capacitive behavior and excellent reversibility of the oxide electrode.

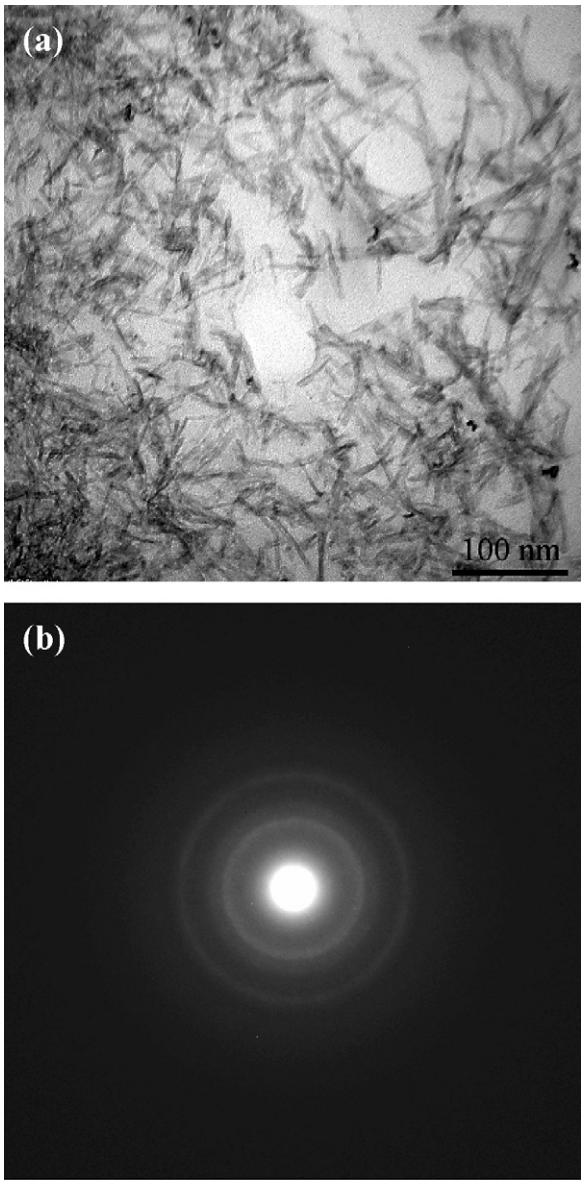

Fig. 2. (a) TEM bright-field image of the manganese oxide prepared by anodic deposition, and (b) its electron diffraction pattern.

In order to explore the energy storage mechanism during the electrochemical process, in situ Mn K-edge X-ray absorption spectroscopic (XAS) study was performed in aqueous 2 M KCl solution. Fig. 4 shows the 21 serial near Mn K-edge XAS spectra of the manganese oxide under a sequence of applied potentials, starting from 0 to 1 V_{SCE} and then back to 0 V_{SCE} with an interval of 0.1 V. Although the spectra did not reveal much difference in the shape, energy shifts of the adsorption peaks were clearly recognized in this figure. More specifically, the peaks gradually shifted toward higher energy with increasing applied potential (scans 1–11) and then backward lower energy as the potential was decreased (scans 11–21). According to literature [15–17], the absorption energy was confirmed to increase with manganese oxidation state. This so-called chemical shift was related to the increase in binding energy of the core-level electron with increasing oxidation state, which is in

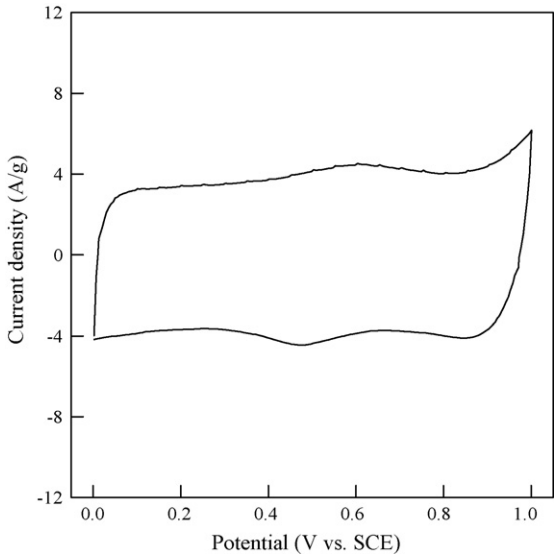

Fig. 3. Cyclic voltammogram of the manganese oxide in 2 M KCl electrolyte at 25 °C with a potential scan rate of 20 mV s^{-1}.

turn caused by the reduced screening of the core level by valence electrons [15]. Therefore, the in situ XAS experimental result, have never been explored in the literature based on our best knowledge, directly confirmed that the faradic redox reaction of manganese oxide indeed occurred during the charge/discharge process. The continuous and reversible change of Mn oxidation state with respect to the applied potential was attributed

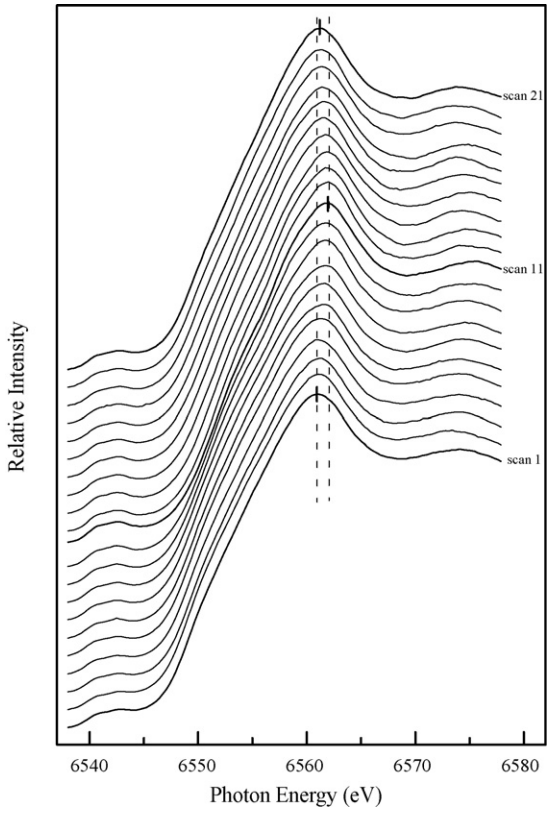

Fig. 4. Twenty-one serial Mn K-edge XAS spectra of the manganese oxide under various applied potentials.

to the nano-crystalline, non-stoichiometric and hydrous natures of the anodically deposited manganese oxide and consequently resulted in demonstrating an ideal pseudo-capacitive performance as characterized in the CV curve of Fig. 3. Moreover, it is noteworthy that since the fluorescence mode was used in the XAS study, the analytical signal was generally collected from a sub-micrometer depth beneath the oxide surface [18]. Accordingly, the experimental result clearly indicated that the faradic redox reaction was not only restricted quite near the surface but also involved within the bulk manganese oxide.

According to literature [15,16], the valence state of Mn can be specifically identified by the absorption threshold energy E_0 which was obtained from the first inflection point on the main absorption edge. Four reference compounds Mn(0), MnO(II), Mn_2O_3(III) and MnO_2(IV), which were also analyzed in our XAS study showed their E_0 values of 6539.0, 6544.7, 6548.2 and 6552.6 eV, respectively. The analytic results clearly revealed the approximately linear relationship between the Mn oxidation state and the E_0. The E_0 values of various XAS scans (shown in Fig. 4) are listed in Table 1. The oxidation states of Mn under various applied potentials can be calculated on the basis of the above-mentioned linear relationship, and the obtained data are also summarized in Table 1. The as-deposited manganese oxide, established an open circuit potential (OCP) of 0.45 V_{SCE}, showed an E_0 value of 6550.6 eV corresponding to a Mn oxidation state of +3.55. Once the potential of 0 V_{SCE} was applied, the oxidation state of Mn was reduced to +3.23. Then, as the potential was raised to 1 V_{SCE} step by step, the Mn oxidation state progressively increased to +3.95. Moreover, the oxidation state of Mn was again gradually reduced to +3.27 as the applied potential was moved backward to 0 V_{SCE}. It is found that the shift of Mn oxidation state within the potential range of 1 V was about 0.7. Accordingly, an ideal specific capacitance of the manganese oxide, based on the active material of $MnO_{3.55/2}$, should be around 800 F g^{-1}. However, practical capacitances of the anodically deposited manganese oxides reported in literature [7,13,14,19,20] were typically 200–300 F g^{-1}. The fact can be associated with two considerations. First, electronic and ionic conductivity of the manganese oxide was not quite satisfactory [6,12,21,22] and thus kinetically limited the high-rate faradic redox reaction within the bulk material. Since the XAS study was performed under a potentiostatic condition (about 1 h for every scan) allowing a much longer reaction period than that of practical applications, the higher obtained specific capacitance was expectable. Second, the anodically deposited produce, besides manganese oxide, was also composed of hydroxide, trapped oxygen, structural water, other impurities, etc. [23]. Some of the species did not participate the faradic redox reaction, consequently resulting in reduction of the specific capacitance.

Fig. 5 summarizes the variation of Mn oxidation state (or E_0) during the electrochemical charge–discharge cycle. The potential-dependence Mn oxidation state was clearly demonstrated. However, a hysteresis loop, presenting a delay of the oxidation state adjustment with respect to the applied potential, can be evidently recognized in this figure. The experiment data pointed out that the valence of Mn had not yet reached the

Table 1
E_0 values and the corresponding Mn oxidation states of the manganese oxide taken from the serial XAS scans performed under various applied potentials. The E_0 values of four reference compounds Mn, MnO, Mn_2O_3 and MnO_2 are also shown

Sample	Potential (vs. SCE)	Scan sequence	E_0 (eV)	Oxidation state
As-deposited manganese oxide	With OCP at 0.45 V		6550.6	3.55
The deposited manganese oxide under various applied potentials	0 V	1	6549.2	3.23
	0.1 V	2	6549.3	3.25
	0.2 V	3	6549.4	3.27
	0.3 V	4	6549.6	3.32
	0.4 V	5	6549.8	3.36
	0.5 V	6	6550.1	3.43
	0.6 V	7	6550.4	3.50
	0.7 V	8	6550.7	3.57
	0.8 V	9	6551.0	3.64
	0.9 V	10	6551.5	3.75
	1.0 V	11	6552.4	3.95
	0.9 V	12	6552.3	3.93
	0.8 V	13	6552.0	3.86
	0.7 V	14	6551.7	3.80
	0.6 V	15	6551.5	3.75
	0.5 V	16	6551.2	3.68
	0.4 V	17	6550.9	3.61
	0.3 V	18	6550.4	3.50
	0.2 V	19	6550.0	3.41
	0.1 V	20	6549.7	3.34
	0 V	21	6549.4	3.27
Mn			6539.0	0
MnO			6544.7	2
Mn_2O_3			6548.2	3
MnO_2			6552.6	4

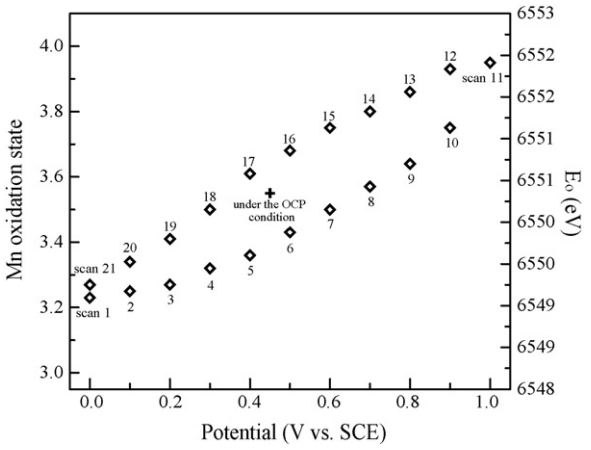

Fig. 5. Dependences of the Mn oxidation state and the E_0 on the applied potential during the electrochemical redox cycle.

steady state even though the every XAS scan was performed under potentiostatic condition for about 1 h, revealing the poor electronic and ionic conductivity of the manganese oxide. This result well supported the above-mentioned hypothesis that considered the unsatisfactory conductivity of the manganese oxide was the crucial factor significantly limited itself from delivering the ideal pseudo-capacitance, especially in high-powder applications. Additionally, it is noticed that the E_0 of the 21st XAS scan is higher than that of the first one as shown in Fig. 5. Clearly, the Mn oxidation state did not completely recover but increased from +3.23 to +3.27 after the electrochemical redox cycle. The irreversibility of the Mn valence state evidently explained the capacitance decay phenomenon of the manganese oxide after cycling which was commonly reported in literature [6,8,19–25].

4. Conclusions

In situ XAS study of the anodically deposited manganese oxide under various applied potentials was demonstrated for the first time in this investigation, revealing the energy storage mechanism of the oxide in 2 M KCl aqueous solution. The pseudo-capacitive performance of the manganese oxide was evidently attributed to the continuous and reversible change in Mn oxidation state, from +3.23 to +3.95 and then back to +3.27, within the potential cycled range of 0–1 V_{SCE}. Moreover, hysteresis of Mn oxidation state adjustment with respect to the applied potential was clearly recognized, elucidating the poor conductivity of the oxide which could limit itself from approaching the ideal pseudo-capacitance. In addition, the incomplete recovery of the Mn oxidation state (from +3.23 to +3.27) after the electrochemical redox cycle was considered to be a reason for capacitance decay of the oxide electrode during charge–discharge process.

Acknowledgement

The authors would like to thank the National Science Council of the Republic of China for financially supporting this research under Contract No. NSC 94-2216-E-006-020.

References

[1] R. Kötz, M. Carlen, Electrochim. Acta 45 (2000) 2483–2498.
[2] B.E. Conway, J. Electrochem. Soc. 138 (1991) 1539–1548.
[3] J.P. Zheng, J. Huang, T.R. Jow, J. Electrochem. Soc. 144 (1997) 2026–2031.
[4] M. Ishikawa, M. Morita, M. Ihara, Y. Matsuda, J. Electrochem. Soc. 141 (1994) 1730–1734.
[5] H.Y. Lee, J.B. Goodenough, J. Solid State Chem. 144 (1999) 220–223.
[6] S.C. Pang, M.A. Anderson, T.W. Chapman, J. Electrochem. Soc. 147 (2000) 444–450.
[7] C.C. Hu, T.W. Tsou, Electrochem. Commun. 4 (2002) 105–109.
[8] S.C. Pang, M.A. Anderson, J. Mater. Res. 15 (2000) 2096–2106.
[9] S. Wen, J.W. Lee, I.H. Yeo, J. Park, S.I. Mho, Electrochim. Acta 50 (2004) 849–855.
[10] M. Toupin, T. Brousse, D. Bélanger, Chem. Mater. 14 (2002) 3946–3952.
[11] M. Toupin, T. Brousse, D. Bélanger, Chem. Mater. 16 (2004) 3184–3190.
[12] M. Nakayama, A. Tanaka, Y. Sato, T. Tonosaki, K. Ogura, Langmuir 21 (2005) 5907–5913.
[13] J.K. Chang, W.T. Tsai, J. Electrochem. Soc. 150 (2003) A1333–A1338.
[14] J.K. Chang, W.T. Tsai, J. Appl. Electrochem. 34 (2004) 953–961.
[15] M. Belli, A. Scafati, A. Bianconi, S. Mobilio, L. Palladino, A. Reale, E. Burattini, Solid State Commun. 35 (1980) 355–361.
[16] P. Ghigna, G. Flor, G. Spinolo, J. Solid State Chem. 149 (2000) 252–255.
[17] S. Quartieri, M.P. Riccardi, B. Messiga, F. Boscherini, J. Non-Cryst. Solids 351 (2005) 3013–3022.
[18] H.B. Garg, E.A. Stern, D. Norman, X-ray Absorption in Bulk and Surfaces, World Scientific Publishing Co., Singapore, 1994.
[19] C.C. Hu, T.W. Tsou, Electrochim. Acta 47 (2002) 3523–3532.
[20] C.C. Hu, C.C. Wang, J. Electrochem. Soc. 150 (2003) A1079–A1084.
[21] H.Y. Lee, S.W. Kim, H.Y. Lee, Electrochem. Solid State Lett. 4 (2001) A19–A22.
[22] J.K. Chang, C.T. Lin, W.T. Tsai, Electrochem. Commun. 6 (2004) 666–671.
[23] J.K. Chang, Y.L. Chen, W.T. Tsai, J. Power Sources 135 (2004) 344–353.
[24] Y.U. Jeong, A. Manthriram, J. Electrochem. Soc. 149 (2002) A1419–A1422.
[25] S. Devaraj, N. Munichandraiah, Electrochem. Solid State Lett. 8 (2005) A373–A377.